

Traction Control of Electric Vehicle

-Basic Experimental Results using the Test EV "UOT Electric March"-

Yoichi Hori, Yasushi Toyoda and Yoshimasa Tsuruoka
Department of Electrical Engineering, University of Tokyo,
7-3-1 Hongo, Bunkyo, Tokyo 113, JAPAN
Tel: +81-3812-2111 ext.7680, Fax: +81-3-5800-3865
E-mail: hori@hori.t.u-tokyo.ac.jp

Abstract : The most distinct advantage of electric vehicle is its quick and precise torque generation. However, most electric vehicles developed until now have not yet utilized it. In this paper, two novel traction control techniques of electric vehicle using this advantage are proposed. One is the model following control and another is the optimal slip ratio control. The basic effectiveness of the proposed methods is demonstrated by real experiments using the DC motor driven test vehicle "UOT (University of Tokyo) Electric March".

Keywords : electric vehicle, motion control, traction control, ABS, model following control, slip ratio control, estimation, robust control, road condition estimation

I. INTRODUCTION

Recently a lot of electric vehicles (EV) have been developed [1] mainly to solve environmental and energy problems caused by the use of internal combustion engine vehicles (ICV). Some of them already have enough performance even in practical use. However, they have not yet utilized the most remarkable advantage of EV. The generated torque of electric motors can be controlled much more quickly and precisely than that of internal combustion engines.[13] It is well known that the adhesion characteristics between tire and road surface are greatly affected by the control of traction motor. This means that the vehicle stability and safety can be greatly improved by controlling the motor torque appropriately. If we can use special low drag tires with smaller energy loss, the range of one battery charge will be drastically expanded.

In this paper, we will propose some novel traction control techniques, which can be firstly realized only by utilizing electric motor's quick torque response. [14] They are the model following control and the optimal slip ratio control. By using a newly developed DC motor driven test vehicle "UOT Electric March", we will show some successful experimental results. In order to achieve the best control performance, the estimation method of road surface condition is proposed and its basic realizability is shown by real experiments

II. STATE-OF-THE-ART OF TRACTION CONTROL

Traction control is the control to suppress tire slip when the vehicle is accelerating on icy road, for example. It is realized by controlling the traction force. As the result, driving and cornering performances are improved.

We should consider two forces acting on the vehicle body. They are the driving (longitudinal) and side (lateral) forces. [2] As depicted in Fig.1, these force characteristics strongly depend on the slip ratio λ . In acceleration, λ is defined by eq.(1), where V_w and V are the wheel and vehicle speeds.

$$\lambda = (V_w - V) / V_w \quad (1)$$

The side force takes its maximum value when $\lambda=0$ and becomes quickly smaller for bigger λ . If λ increases by sudden decrease of road friction, the side force gets smaller drastically. This causes serious problems: drift-out in front wheel driven cars, spin in rear wheel driven cars, and drift-out with rotation in four wheel driven cars. Such a loss of cornering force is extremely dangerous. The average traction force is also decreased.

We think that the traction control can be classified into the following two steps:

(1) **longitudinal control**, for example, the adhesion improvement control to prevent slip. This is done by controlling the traction force,

and

(2) **lateral control**, for example, the yaw control to keep the yaw motion to be zero. At present, this is done mainly by controlling the steering angle.

For the lateral control, the steering angle of the front wheels is the dominant control input. [3][4][5] Such a technique is already well developed for ICV. Most results of them can be applied to EV in a much more sophisticated manner. For example, by introducing the independent control of 4 in-wheel motors, we can realize completely new motion control of EV. [6][7] However, in this paper, as our first attempt, we focus our discussion into (1) **longitudinal control**.

To realize the effective traction control system, we need a sophisticated mechanism quickly to reduce the excessive driving torque. In ICV, this is realized mainly by the following three techniques.

(1) **engine control**: Engine torque itself is suppressed. To reduce air supply is the basic technique, but for quicker response, advanced techniques like fuel-cut and spark timing shift are used together.

(2) **brake control**: Wheel rotation itself can be stopped by braking. This method has quicker response than the engine control. Independent control of left and right tires is effective for μ -split braking. Brake control should be used together with the engine control because brake parts often have thermal problem.

(3) **mission control**: Driving torque of the slipping tire is transferred to the non-slipping tire. This technique is effective for μ -split road. As the total torque can not be reduced, this mission control should be applied together with the engine control.

TABLE I summarizes the advantages and disadvantages of these techniques.

III. ADVANTAGE OF ELECTRIC VEHICLE

Electric vehicle has great advantages as followings for realization of high performance traction control.

- (1) **low cost**: In a case of ICV, above mentioned techniques need additional costly hardware, e.g., throttle and brake actuators. EV does not need anything more. Traction control can be realized only by software. Even the lowest cost "basic car" can have high performance traction control.
- (2) **quick response**: In ICV, more than 200[ms] are needed to open the throttle actuator. The actual response is much slower because some more delay in mechanical system must be included. In contrast, the response time of electric motor torque is less than 10[ms].
- (3) **easy controller design**: In ICV, unknown strong non-linearity lies in the transfer characteristics from the control input (for example, air valve angle to engine, oil pressure of brake system, etc.) to the generated torque. This makes it difficult to construct a mathematical model for controller design. In EV, by applying simple current control, the generated torque is exactly proportional to the torque command.

IV. MODEL FOLLOWING CONTROL

In this paper, we propose two control strategies: "**model following control (MFC)**" and "**optimal slip ratio control**". MFC is the starting point of our research project of "control of electric vehicle" and its basic feasibility is demonstrated here by real experiment.

A. Principle of MFC

Fig.2 shows the block diagram of model following control. I_{com} is the current command proportional to the acceleration pedal angle. ω is the rotational speed of the driving shaft. ω increases drastically when the tire slips. Although the vehicle dynamics including tire characteristics and road surface friction are very complicated, if we introduce the slip ratio λ , the vehicle body can be seen as one inertia system having the equivalent inertia moment of

$$J = J_w + Mr^2(1-\lambda) \quad (2)$$

Here, J_w , M and r are the shaft inertia moment, vehicle weight and tire radius. Eq.(2) means that, when slip occurs, the vehicle seems lighter. Therefore, we use the following inertia moment with $\lambda=0$ in the reference model.

$$J_{model} = J_w + Mr^2 \quad (3)$$

When there is no slip, actual J is almost equal to J_{model} . Any signal is not generated from MFC controller. If the tire slips, the actual wheel speed ω increases immediately. The model wheel speed

does not increase. By feeding the speed difference back to the motor current command, the actual motor torque is reduced quickly and it induces re-adhesion.

As this control function is needed only in relatively higher frequency region, we used a high pass filter on the feedback pass. In actual implementation, in order to avoid the offset problem of an integrator, two high pass filters are inserted before taking difference between the actual and the model speeds. When the feedback torque from MFC blocks is positive, it is forced to be zero.

B. Experimental Result of MFC

Fig.3 shows the slip experiment using UOT Electric March. We used iron plates as slippery road surface. Water is scattered to reduce the friction coefficient. The vehicle is accelerated by the constant current command of 300[A]. The feedback gain K in Fig.2 is 30. The front wheels are on the slippery area between $t=1.25[s]$ and $1.7[s]$.

Experimental results are given in Fig.4. We can see that MFC can reduce the motor current effectively when the vehicle goes onto the slippery area, and then the slip ratio is kept much lower comparing to the case of current control only. Some vibration observed in the current waveform in Fig.4(a) can be suppressed in the future.

V. OPTIMAL SLIP RATIO CONTROL

The model following control is a very rough approach although it has been shown that the motor control is really effective for adhesion improvement. If we want more exactly to regulate the slip ratio within the desired range, more precise approach is needed. Fig.5 shows the idea of the optimal slip ratio control developed from this viewpoint. When the optimal slip ratio is decided by the road condition estimator, the slip ratio controller receives the command and tries to realize it.

A. Vehicle Model

We assume that the two motor torques and friction forces are same in left and right, and that the rolling and air frictions are small enough. In Fig.6, the kinematic equations of the wheel and vehicle take the forms of

$$(F_m - F_d) \frac{1}{M_w s} = V_w \quad (4)$$

and

$$F_d \frac{1}{M s} = V \quad (5)$$

where,

- F_m : motor torque (force equivalent)
- F_d : friction force
- M_w : wheel inertia (mass equivalent)
- M : vehicle weight

The friction force between the road and wheel is given by

$$F_d = N \mu(\lambda) \quad (6)$$

where N is the vertical force given by $N = Mg$.

From eq.(1), the following perturbation system is derived.

$$\Delta\lambda = \frac{\partial\lambda}{\partial V} \Delta V + \frac{\partial\lambda}{\partial V_w} \Delta V_w = -\frac{1}{V_{w0}} \Delta V + \frac{V_0}{V_{w0}^2} \Delta V_w \quad (7)$$

where V_{w0} and V_0 are the wheel and vehicle speeds at the operational point. The friction force is represented using a , the gradient of $\mu-\lambda$ curve, as

$$\Delta\mu = a \Delta\lambda \quad (8)$$

By combining eqs.(7) and (8) with the perturbation forms of eqs. (4) and (5), the transfer function from the motor torque to the slip ratio is finally given by

$$\frac{\Delta\lambda}{\Delta F_m} = \frac{1}{Na} \frac{M(1-\lambda)}{M_w + M(1-\lambda)} \frac{1}{1+\tau s} \quad (9)$$

where the time constant τ is given by eq.(10) which is proportional to the wheel speed V_{w0} .

$$\tau = \frac{1}{Na} \frac{MM_w V_{w0}}{M_w + M(1-\lambda)} \quad (10)$$

The typical value of τ in our experimental vehicle is 150 ~ 200[ms] when $a=1$ and the vehicle speed is around 10[km/h]. Note that a can be negative in the right-hand side of the peak point of $\mu-\lambda$ curve.

B. Design of Slip Ratio Controller

We used a simple PI controller with a variable gain as the slip ratio controller given by eq.(11). Its nominator compensates for the pole of eq.(9). The integral gain is constant and the proportional gain is proportional to the vehicle speed.

$$K \frac{1+\tau s}{s} \quad (11)$$

Finally, the transfer function from the slip ratio command to the actual slip ratio becomes

$$\frac{\Delta\lambda}{\Delta\lambda^*} = \frac{1}{1 + Na \frac{M_w + M(1-\lambda)}{M(1-\lambda)} \frac{1}{K} s} \quad (12)$$

If $\lambda \ll 1$, this is a simple first order delay characteristics with a time constant which can be adjusted by K . Here, we put this response time $50 \sim 100$ [ms].

Fig.8 shows the nominal slip ratio used in the slip ratio controller. We defined it by $a=1$. The point of $a=1$ is located just in left side of the peak and is stable. Both of the longitudinal and lateral forces are kept still high.

C. Robustness to Parameter Variation

Because the actual system parameters change widely, we should investigate the robustness of the slip ratio controller. Fig.9 draws the root locus to continuous change of K and a_r (actual a).

From the figures, we can see that the roots move to the left half plane when the controller gain K increases. It is interesting that this controller stabilizes the system even when actual a is negative, although the roots move towards the unstable region.

D. Simulation of Slip Ratio Control

Fig.10 shows the vehicle model we used in the simulation. T represents the motor torque and r the total gear ratio of the drive train. F_d represents the summation of traction force transferred to the contact point of tire and road surface. It is the product of the traction coefficient μ and $N=Mg$, the vertical load on the contact point. μ is defined as the function of λ , which is given by the measured curve shown in Fig.11.

Fig.12 is the simulation result. The response time of the slip ratio controller is set to be 100[ms]. We can see good response characteristics.

E. Experimental Results of Slip Ratio Control

Fig.13 shows the experimental results of the slip ratio control using the laboratory-made experimental electric vehicle "UOT Electric March". Here the response time is 50[ms] and the target slip ratio is 0.1 in Fig.13(a) and is changed stepwise from 0.3 to 0.1 in Fig.13(b).

Basically we can see fairly good performances but there are some problems. First, the actual value of a was much smaller than the nominal value 1. This made the response time longer than the designed value. Next, in Fig.13(b), we see an undershoot to the slip ratio command of 0.1. This is because the motor controller we used is just a 1-quadrant chopper, who can not absorb the motor current.

VI. ESTIMATION OF ROAD CONDITION

In the previous chapter, we showed the effective slip ratio control. Next problem is how to give the optimal slip ratio to the slip ratio controller.

We showed the relation between the slip ratio λ and the friction coefficient μ in Figs.1 and 11, but it varies very widely according to road surface condition as shown in Fig.14. It is clear that the slip ratio where the friction force takes its maximum value vary according to road condition. This means that road condition should be estimated relatively quickly for giving the optimal slip ration to the slip

ratio control.

To know the road surface condition, we should estimate the friction coefficient.[10]-[12] If we can measure the vehicle speed directly by using non-driven wheel, the friction coefficient μ can be obtained by eq.(13) based on eqs.(3) and (4).

$$\mu = \frac{M}{N} \frac{dV}{dt} \quad (13)$$

When the vehicle speed can not be measured directly, we can estimate μ based on eq.(14).

$$\mu = \frac{1}{N} \left(F_m - M_w \frac{dV_w}{dt} \right) \quad (14)$$

In our case, we can use both of these two methods. Fig.15 shows the estimation result of μ - λ curve of dry asphalt road when no slip control is active. At the point around $\lambda=0.08$, the gradient a of μ - λ curve is about 1.

Fig.16 shows the estimation results on wet iron surface under the slip ratio control proposed in the previous chapter. Here, the optimal slip ratio is smaller than 0.05. It is also noticed that, in our experiment shown in Fig.13(a), the actual gradient of μ - λ curve at $\lambda=0.1$ was almost -1. We can see that the slip ratio controller works still effectively even when the operation point is unstable, but, in this case, we should have commanded a lower slip ratio.

For effective traction control, it is enough to know the gradient of μ - λ curve. We are going to introduce an adaptive identification method for realization of "the optimal slip ratio control based on the estimation of road surface condition", which is our next target.

VII. CONCLUSION

We propose a new field of "Motion Control of Electric Vehicle". EV is a very interesting object combining electrical and mechanical engineering fields from the viewpoint of motion control. As an example, we proposed advanced adhesion control utilizing quick and precise torque response of electric motor.

We proposed the Model Following Control and the Optimal Slip Ratio Control. We confirmed that MFC can reduce its torque quickly when the motor speed is suddenly increased by tire slip. Next, we showed that the optimal slip ratio control has more advanced performance. Such kinds of quick controls are firstly realized only in electric vehicles. It is clearly shown that relatively sophisticated control theory can work well in actual experiments.

Advanced adhesion control is helpful for lateral control like yaw disturbance attenuation.[6]-[9] This is because the proposed optimal slip ratio control keeps the tire slip within the small region where both of the longitudinal and lateral adhesion coefficients are still high enough.

ACKNOWLEDGEMENT

The authors would like to express their sincere thanks to Mr. Furuya in Kansai Electric Power Company for his big work on Electric March when he was a graduate student in our laboratory. They also thank Mr. Uchida and Mr. Yamazaki for their help in manufacturing of the vehicle.

APPENDIX

Configuration of UOT Electric March

We developed a real test electric vehicle "UOT Electric March" seen in Fig.A-1. It is a convert car, whose IC engine is replaced by an electric motor.

The front two wheels are driven by a 19[kW] series-wound DC motor through a 5 speed manual transmission and a differential gear. The 1-quadrant DC chopper supplies power to the motor. Its current limit is 400[A] and can produce maximum torque over 100[Nm], which is enough to perform the slip experiment. Current and speed sensors are also implemented. To detect the vehicle speed, a speed sensor is implemented in the rear wheel.

The aim of our research is not in motor control itself, but in motion control of electric vehicle, where the kind of motors is not a problem. What is required for the traction motor is to generate torque quickly enough. Our development is based on this quick and relatively precise torque generation. From this point of view, DC motor is the easiest device to confirm our idea, in particular, for basic experiment in a university.

Fig.A-2 shows the control system of the vehicle and TABLE A-I gives its specification. We used a note-type personal computer to realize all control algorithms. It not only executes the control algorithm and puts out the voltage command to the chopper, but also reads and records the sensor data. As the control algorithms are written by software (C-language), we can easily investigate various control strategies.

Fig.A-3 shows the basic experimental results of the current controller.

REFERENCES

- [1] K. Rajashekara, "History of Electric Vehicles in General Motors", *IEEE Trans. on Ind. Appl.*, Vol.30, No.4, pp.897-904, July/August 1994.
- [2] Hideo Sakai, "Tire Engineering", *Grand-Prix Pub. Co.*, 1987.
- [3] M.Ito and K. Isoda, "The Present and Future Trends of Traction Control System", *Jidosha-Gijutsu, Society of Automotive Engineers of Japan*, Vol.46, No.2, pp.32-37, 1992.
- [4] K. Ise, et. al., "The 'Lexus' Traction Control (TRAC) System", *SAE (Society of Automotive Engineers of Japan) Technical Paper*, No. 900212, 1990.
- [5] S. Yamazaki, T. Fujikawa and I. Yamaguchi, "A Study on Braking and Driving Properties of Automotive Tires", *Transactions of the Society of Automotive Engineers of Japan*, Vol.23, No.2, pp.97-102, 1992.
- [6] J. Ackermann, "Yaw Disturbance Attenuation by Robust Decoupling of Car Steering", *Proc. of 13th IFAC World Congress*, 8b-01-1, pp.1-6, 1996.
- [7] Y. Wang and M. Nagai, "Integrated Control of Four-Wheel-Steer and Yaw Moment to Improve Dynamic Stability Margin", *Proc. 35th IEEE-CDC*, pp.1783-1784, 1996.
- [8] N. Iwama, et. al., "Active Control of an Automobile -Independent Rear Wheel Torque Control-", *Transactions of SICE*, Vol.28, No.27, pp.844-853, 1992.
- [9] S.K.Sul and S.J. Lee, "An Integral Battery Charger for Four-Wheel Drive Electric Vehicle", *IEEE Trans. on Ind. Appl.*, Vol.31, No.5, September/October 1995.
- [10] C. Liu and H. Peng, "Road Friction Coefficient Estimation for Vehicle Path Prediction", *Vehicle System Dynamics Supplement*, 25, pp.413-425, Swets & Zeitlinger, 1996.
- [11] A. Daiss and U. Kiencke, "Estimation of Tire Slip during combined Cornering and Braking Observer Supported Fuzzy Estimation", *Proc. of 13th IFAC World Congress*, 8b-02-2, pp.41-46, 1996.
- [12] L. R. Ray, "Nonlinear Tire Force Estimation and Road Friction Identification: Simulation and Experiments", *Automatica*, Vol.33, No.10, pp.1819-1833, 1997.
- [13] T. Furuya, Y. Toyoda and Y. Hori, "Implementation of Advanced Adhesion Control for Electric Vehicle", *Proc. IEEE Workshop on Advanced Motion Control (AMC-Mie'96)*, Vol.2, pp.430-435, 1996.
- [14] Yoichi Hori, Yasushi Toyoda and Yoshimasa Tsuruoka, "Traction Control of Electric Vehicle based on the Estimation of Road Surface Condition -Basic Experimental Results using the Test EV UOT Electric March-", *Proc. IEEJ-IEEE Power Conversion Conference (PCC-Nagaoka '97)*, Vol.1, pp.1-8, 1997.

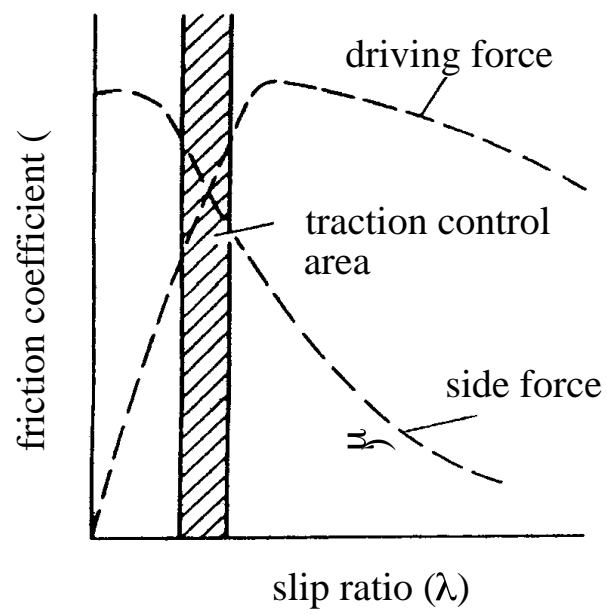


Fig.1. Characteristics of driving and lateral forces.

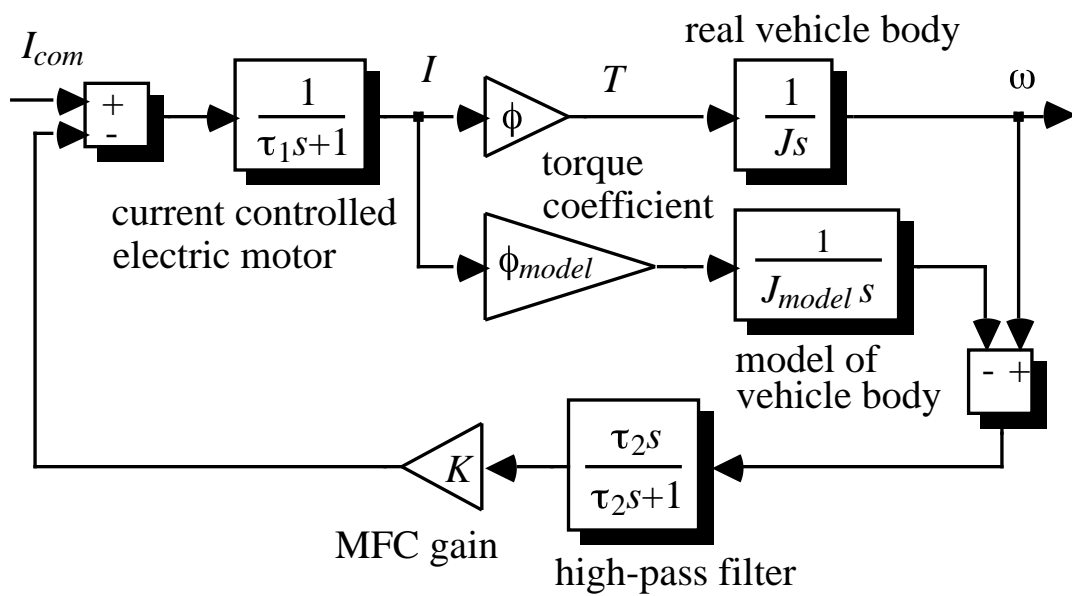


Fig.2. Block diagram of MFC.

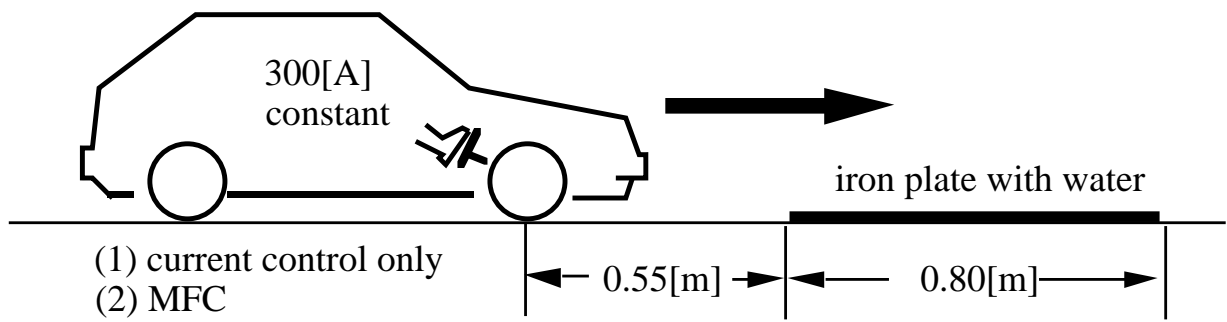
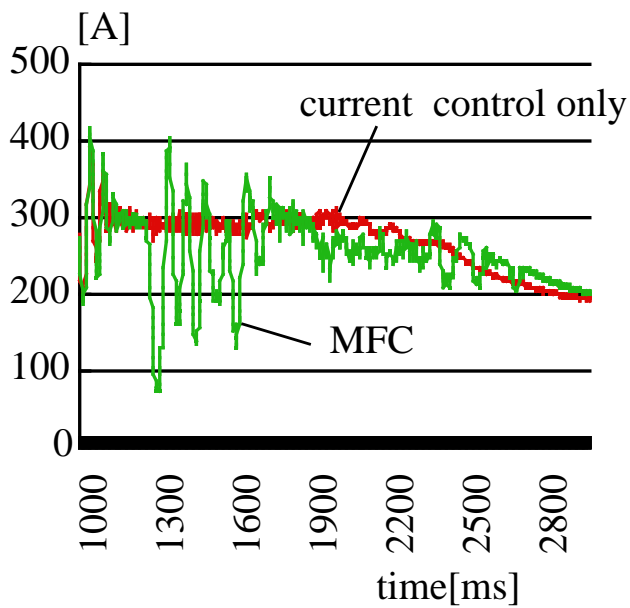
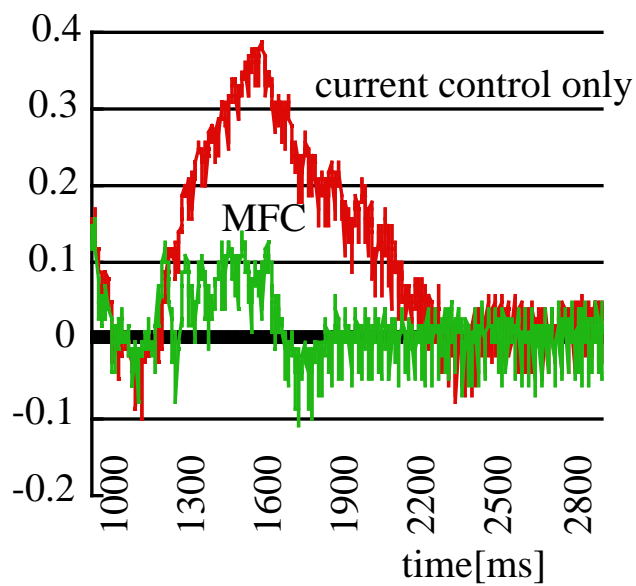


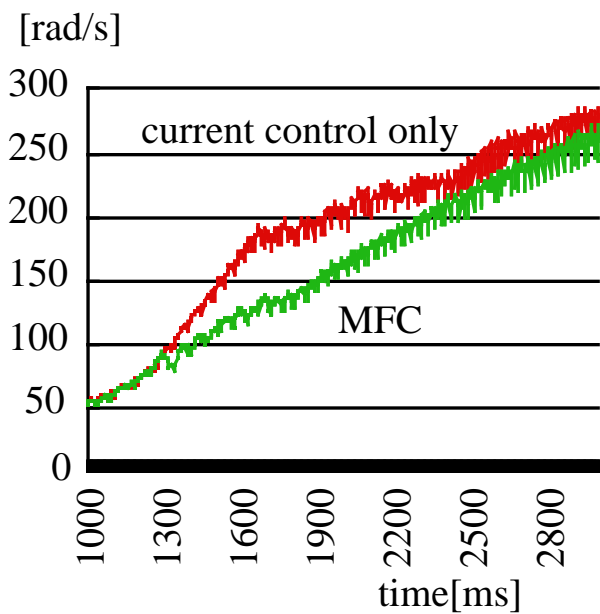
Fig.3. Slip experiment.



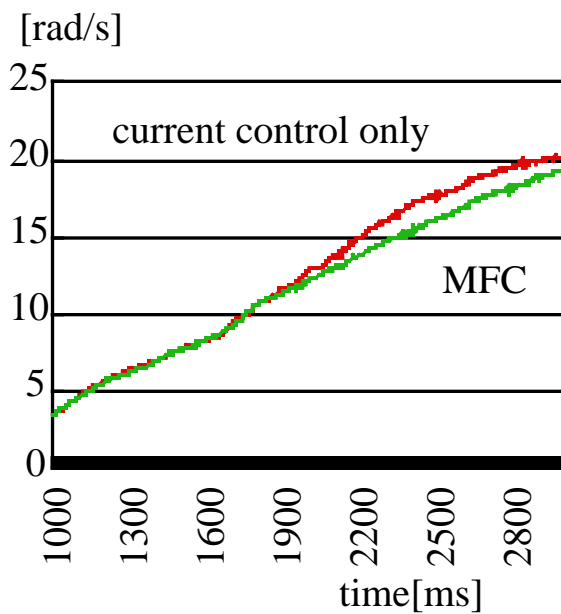
(a) motor current



(b) slip ratio



(c) wheel speed



(d) vehicle speed

Fig.4. Experimental results of MFC.

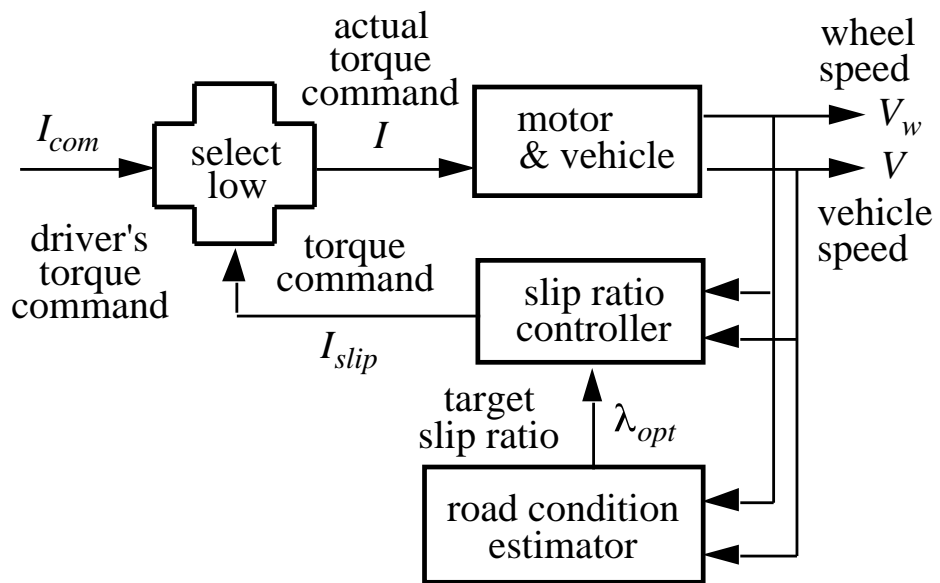


Fig.5. Block diagram of the optimal slip ratio controller.

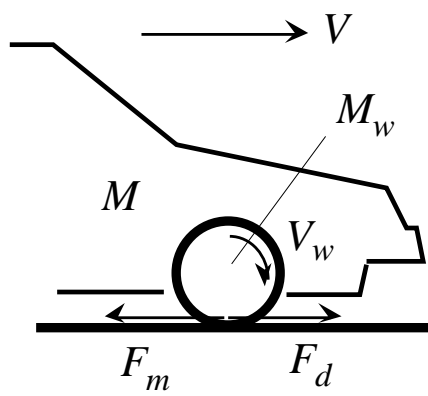


Fig.6. Vehicle model.

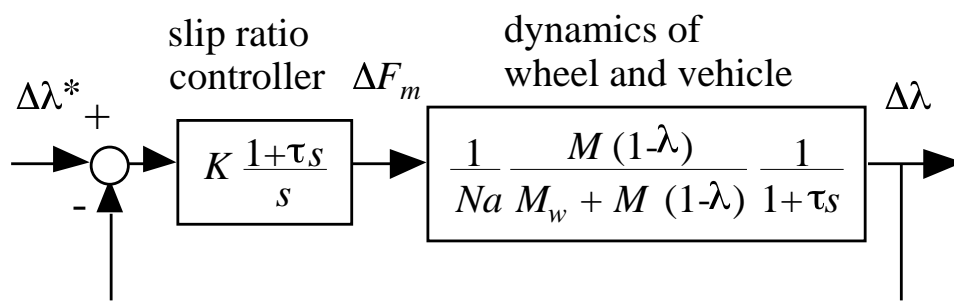


Fig.7. Slip ratio controller.

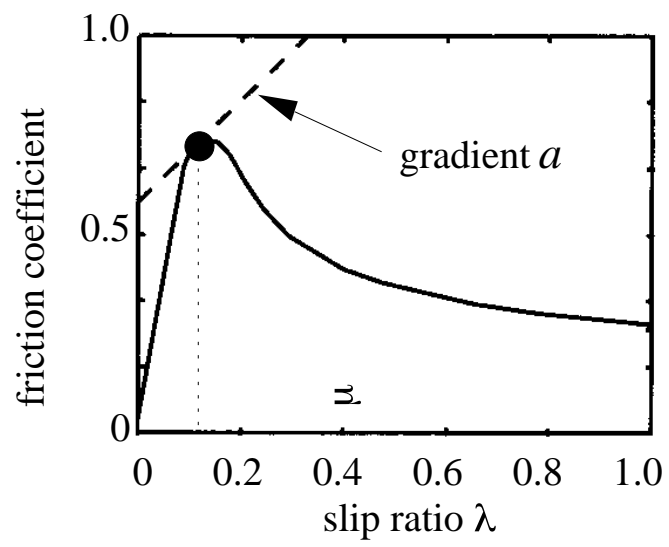


Fig.8. Nominal slip ratio is given by $a=1$.

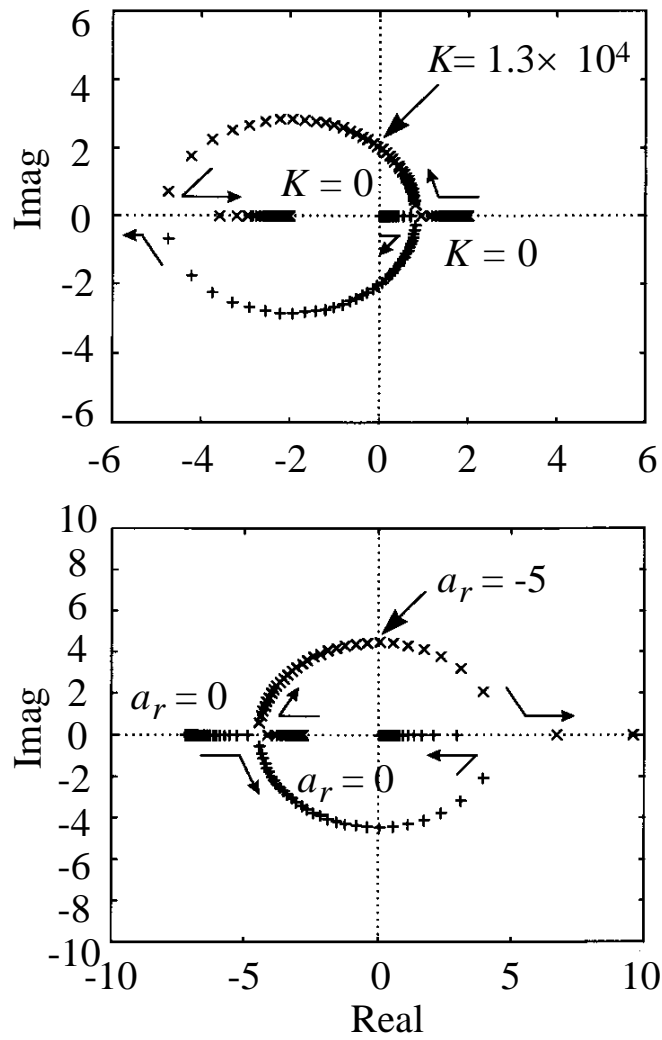


Fig.9. Root locus against parameter variation.

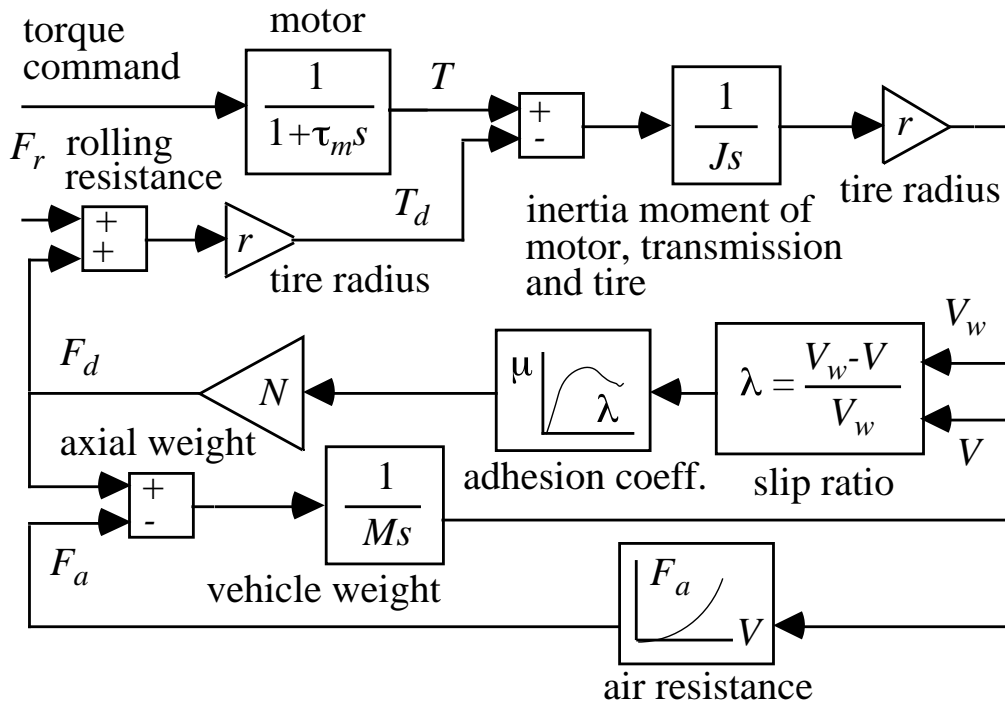


Fig.10. Vehicle model used in the simulation.

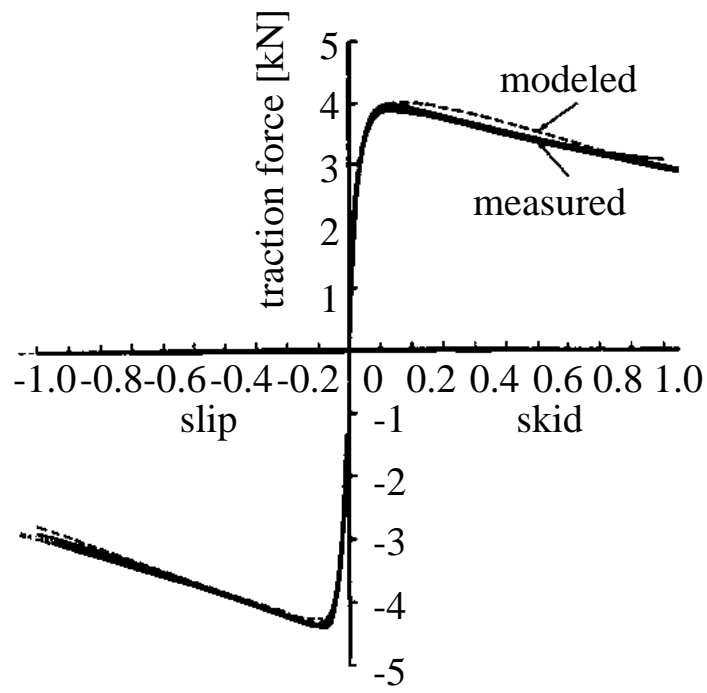


Fig.11. μ - λ characteristics used in the simulation.

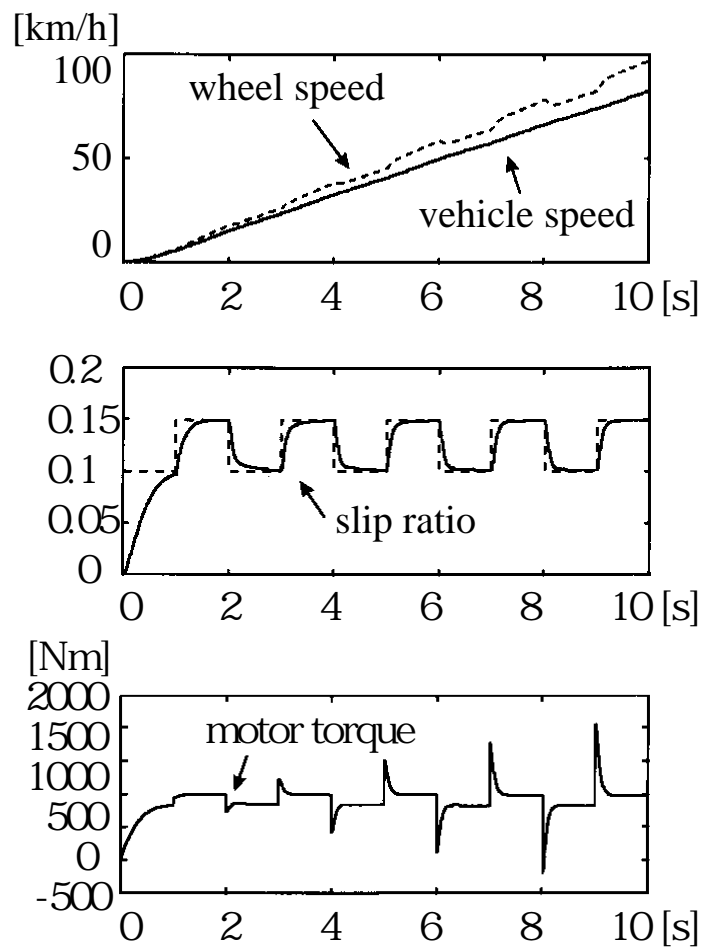
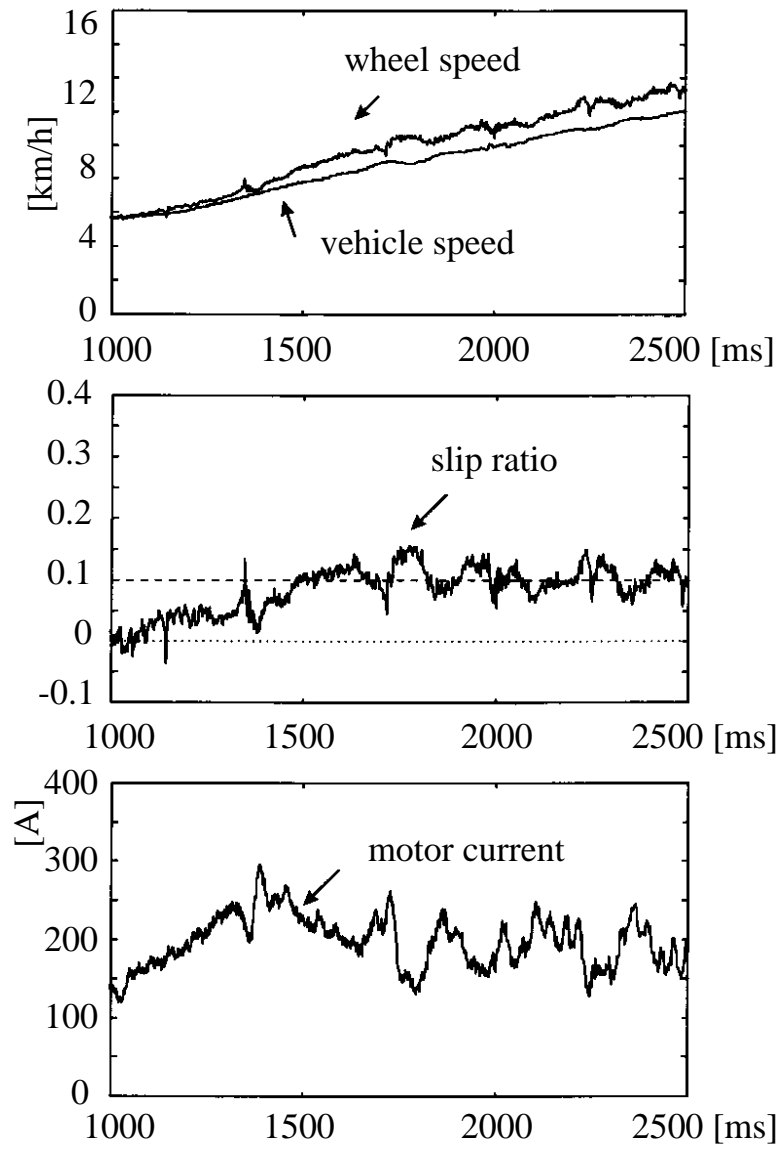
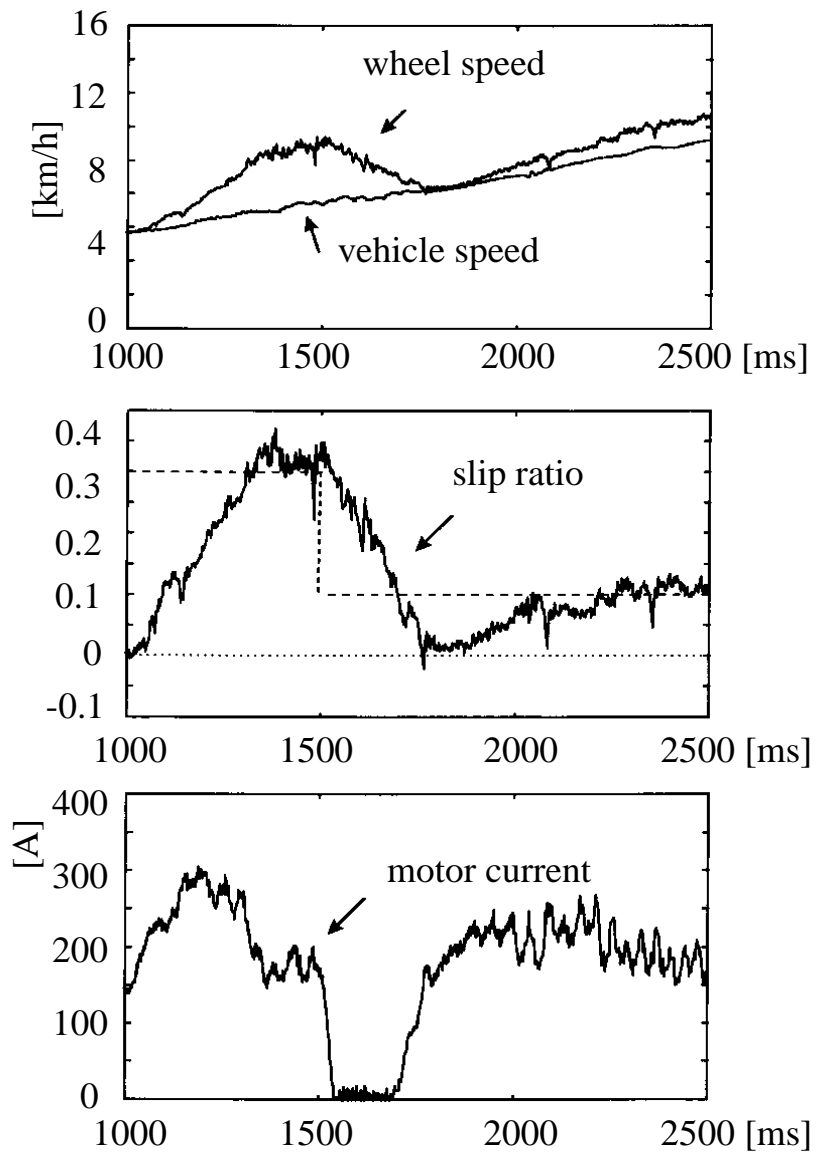


Fig.12. Simulation of the slip ratio control.



(a) constant slip ratio command

Fig.13. Experimental results of the slip ratio control.



(b) changing slip ratio command

Fig.13. Experimental results of the slip ratio control.

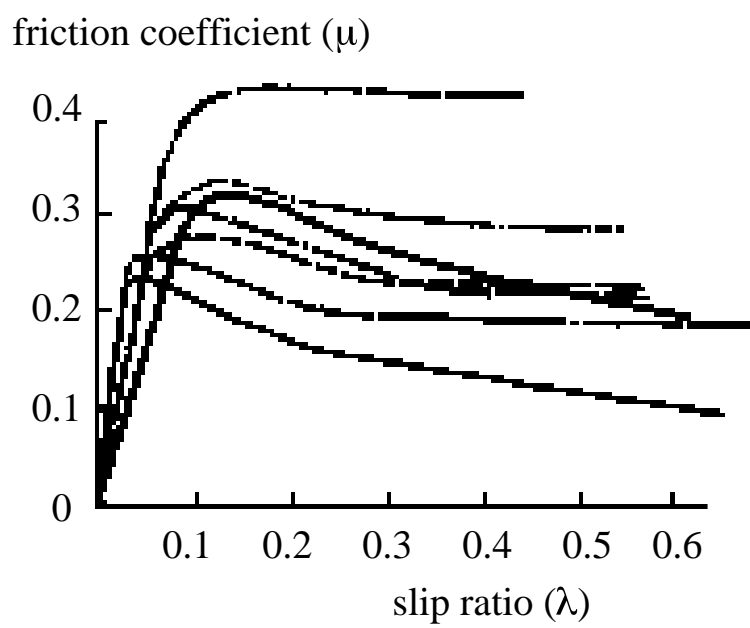


Fig.14. Various Road Condition.
(Actual explanation of each curves is omitted.)

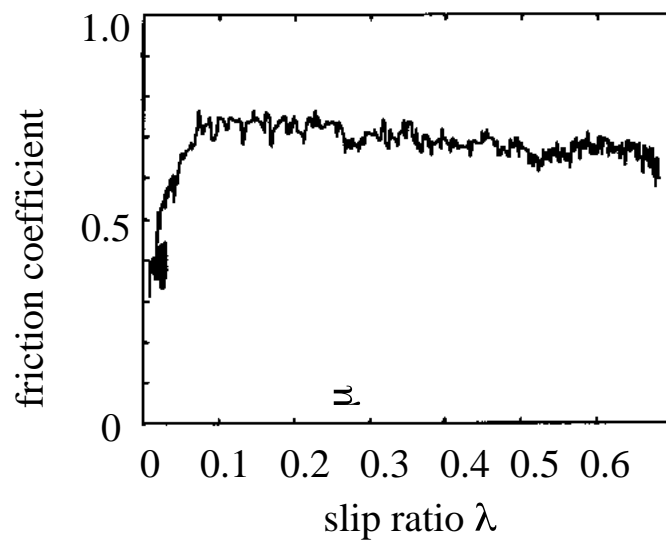


Fig.15. Estimation result of μ - λ curve of dry asphalt road.

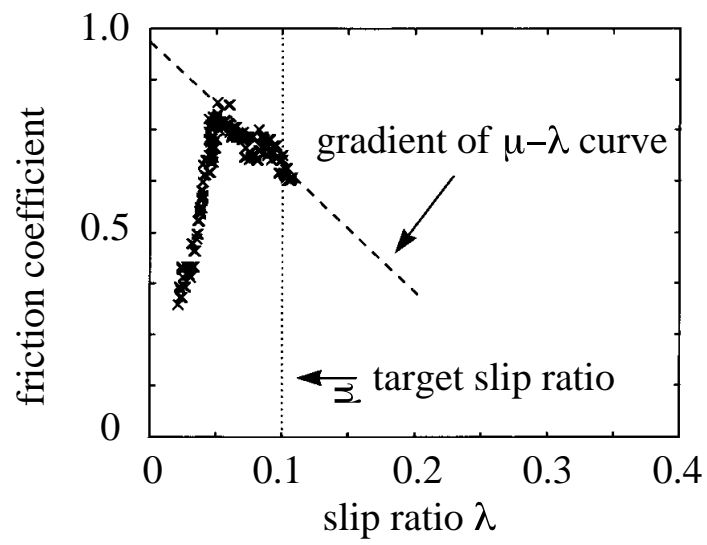


Fig.16. Estimation result of $\mu-\lambda$ curve of wet iron plate under the slip ratio control.



Fig.A-1. UOT Electric March.

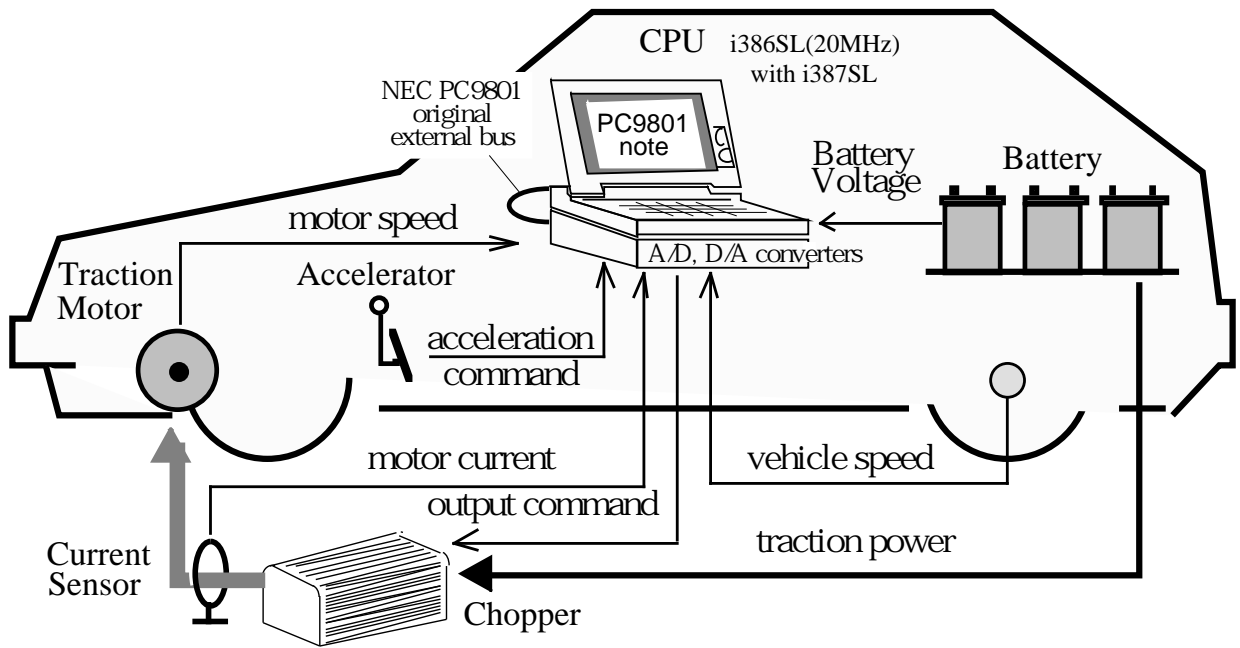


Fig.A-2. Configuration of UOT Electric March.

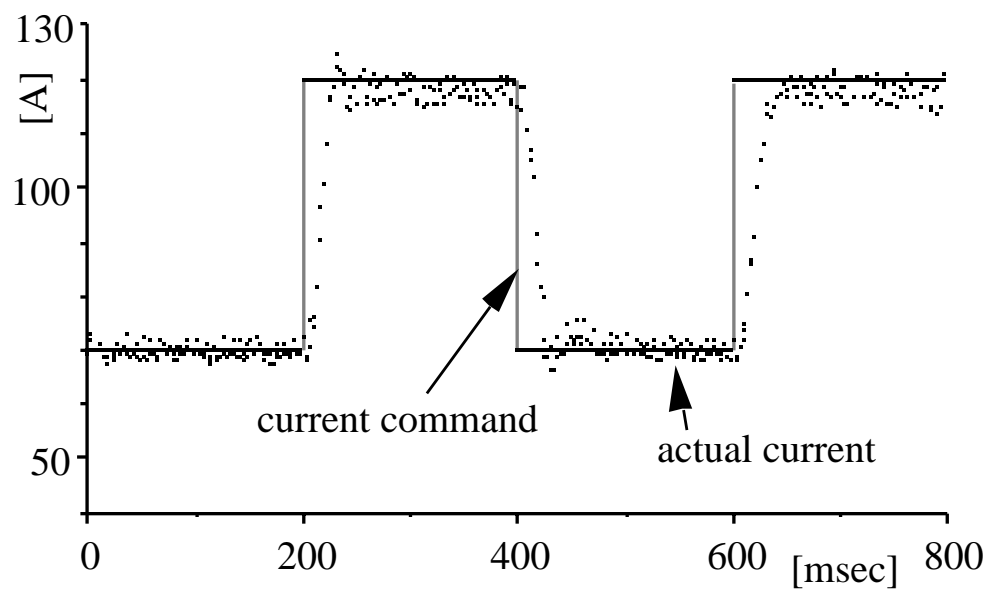


Fig.A-3. Basic experiment on the current response.

TABLE I
COMPARISON OF TRACTION CONTROLS FOR ICV

	controllability	response	cost	operation feeling	total
engine control	good	fair	excellent	fair	good
brake control	good	excellent	excellent	poor	fair
mission control	fair	poor	excellent	fair	poor
engine + mission controls	good	fair	good	fair	fair
engine + brake controls	excellent	excellent	good	good	excellent

TABLE A-I
SPECIFICATION OF UOT ELECTRIC MARCH

Conversion Base	Nissan March (Micra)
size	3785 × 1560 × 1395[mm]
weight	900[kg](batteries included)
Motor	Advanced D.C. Motors, Inc.
type	DC series wound
rated power (@120V)	19[kW](1hr.), 32[kW](5min.)
size/weight	φ 232, length 397[mm], 65[kg]
Controller	Curtis Instruments, Inc.
type	MOSFET PWM Chopper
operating frequency	15[kHz]
rated voltage/current	120[V]/400[A]
Battery	Japan Storage Battery Co.,Ltd. GTX-130E41L
type	lead acid
voltage/capacity	72[V]/92[Ah](5hr)
weight	27.5[kg] × 6
CPU	PC9801NS/T (386SL, 20MHz)
weight	3.2[kg]
A/D and D/A converters	12bit, 8ch / 12bit, 2ch